

# Electrochemical Methoxylation of an HF-Etched Porous Silicon Surface

James L. Gole\*

*School of Physics, Georgia Institute of Technology, Atlanta, Georgia 30332-0430*

David A. Dixon\*

*Environmental Molecular Sciences Laboratory, Pacific Northwest National Laboratory, P.O. Box 999, K1-83, Richland, Washington 99352*

*Received: November 10, 1997; In Final Form: January 7, 1998*

The electrochemical methoxylation of a porous silicon (PS) surface using an anhydrous methanol etch and the resulting modification of the photoluminescent emission (PL) from the surface are evaluated within the framework of the silanone-based silicon oxyhydride fluorophors and their methylated counterparts. The molecular electronic structure of the ground-state singlet and low-lying triplet electronic states of some 20 oxyhydrides of the form  $\text{O}=\text{Si}(\text{R})_2$ ,  $\text{O}=\text{Si}(\text{R})\text{OR}$ , and  $\text{O}=\text{Si}(\text{OR})_2$ , where  $\text{R} = \text{H}$ ,  $\text{CH}_3$ , or  $\text{SiH}_3$ , is considered. The predicted electronic transitions correlate well with the experimentally observed PL for PS and its methoxylated counterpart. The substitution of a methyl ( $\text{CH}_3$ ) group for a silyl ( $\text{SiH}_3$ ) unit is predicted to produce the observed PL blue shift accompanied by an increased PL intensity and stability.

## Introduction

High surface area porous silicon (PS) structures formed in wafer scale through electrochemical etching display a visible photoluminescence (PL) upon excitation (PLE) with a variety of visible and ultraviolet light sources.<sup>1–3</sup> This room-temperature luminescence has attracted considerable attention primarily because of its potential use in the development of silicon-based optoelectronics, displays, and sensors. Under the appropriate conditions, PS displays a “green” luminescence during the early and intermediate stages of the etching process. The green luminescence then transforms to a final “orange-red” luminescence (600–800 nm), although it can be stabilized for extended periods with appropriate solvation.<sup>4–6</sup> We have recently carried out a detailed quantum chemical study which, coupled with experiment,<sup>5</sup> suggests that plausible sources of the PS green and orange-red photoluminescent emissions are the silanone-based silicon oxyhydrides strongly bound to the PS surface and that the transformation corresponds to an oxidation cycle involving these oxyhydrides. Here, we again use detailed quantum chemistry to examine the derivatization of the PS surface with the goal of enhanced stability, increased quantum yield for light emission, and the consideration of a protocol for sensor applications. We thus focus on the methoxylation of the PS surface as recently characterized by Warntjes et al.<sup>7</sup>

While the luminescence from PS is thought to occur near its surface,<sup>8</sup> the source of the visible emission is controversial, as the efficiency and wavelength range of the emitted light can be affected by the physical and electronic structure of the surface, the nature of the etching solution, and the nature of the environment into which the etched sample is placed.<sup>3–6</sup> The stabilization of PS and the conservation of its luminescence efficiency represent challenges that might be solved through the derivatization of the surface. In fact, the methoxylations of the surfaces of flat silicon crystals are reported to be key factors accounting for long-term stability and low interfacial recombination characteristics in methanol-based photoelectro-

chemical cells.<sup>9</sup> Therefore, such modifications of a PS surface are attractive in that they might provide increased stability either for device applications or as a test of fundamental models that attempt to explain the luminescence mechanism.

The luminescence from PS has been attributed to quantum-confined electrons and holes in columnar structures or undulating wires,<sup>10–12</sup> surface-localized states,<sup>8,13</sup> and surface-confined molecular emitters.<sup>14–18</sup> Stutzmann and co-workers<sup>15,17</sup> have used the optical detection of magnetic resonance (ODMR) to establish that the PS “red” emission results from a triplet exciton. Identifying the close analogy of both the ODMR and optical excitation (PLE) and photoluminescence spectra of PS and “annealed” siloxene, Stutzmann et al.<sup>15,17</sup> suggested this molecule as the origin of the PS photoluminescence. More recently, we have suggested a correlation with the manifold of electronic states associated with the silanone-based silicon oxyhydrides of the form  $-\text{Si}(\text{O})(\text{OH})$ <sup>5,19</sup> or  $-\text{Si}(\text{O})(\text{OSiH}_3)$ . Changes in bonding associated with electronic transitions involving the oxyhydride ground electronic and low-lying triplet states,<sup>17</sup> especially in the  $\text{SiO}$  related bonds, and the substantial shift to larger internuclear distance of these excited electronic states relative to their ground states can easily explain the observed character of the PL spectra. The excitation to a low-lying triplet state greatly shifted from the ground electronic state partially explains the significant red shift of the PL spectrum (600–800 nm) from the known absorption peak wavelength of the (PLE) excitation spectrum ( $\sim 350$  nm).<sup>20</sup> Further, calculated IR spectra are in excellent agreement with FTIR data.<sup>21</sup>

In the present article, we consider the expected effect of methoxylation and methylation on the PS surface correlating our quantum chemical modeling with the observations of Warntjes et al.<sup>7</sup> We therefore assess changes as we modify the silanone-based oxyhydrides, introducing methyl groups to replace hydrogen and  $\text{SiH}_3$  constituencies.

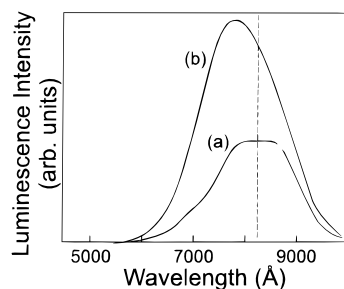


**Figure 1.** Photoluminescence spectra taken for a 2  $\mu\text{m}$  thick 85% porosity PS layer (a) after 60 min aging in 20% aqueous HF, before modification, and (b) after anodic modification in anhydrous methanol @ 10  $\text{mA}/\text{cm}^2$  for 15 s. Spectrum b is considerably more intense and blue shifted. Taken from ref 7.

### Electrochemical Methoxylation of Porous Silicon

Warntjes et al.<sup>7</sup> have developed an electrochemical process to graft methoxy groups onto a PS surface at room temperature employing the partial anodic dissolution of PS in anhydrous methanol. Porous silicon layers were prepared on (100) Si wafers (p-type) using anodization conditions corresponding to a current density of (1) 10  $\text{mA}/\text{cm}^2$  (5 min etch) in 15% aqueous HF or (2) 20  $\text{mA}/\text{cm}^2$  for 2 min in 20% aqueous HF. These layers, of 70–85% porosity and 2  $\mu\text{m}$  thickness, were transferred into 48% aqueous HF, in which they were allowed to age for approximately 30 min. After rinsing in bidistilled water, they were characterized using FTIR and PL spectroscopy (Hg arc lamp, PLE @ 365 nm).

Warntjes et al.<sup>7</sup> have electrochemically modified the standard PS surface in an electrolyte consisting of 0.1 M lithium perchlorate in anhydrous methanol. The modification of the PS surface, performed under galvanostatic conditions in a glovebox in order to maintain the anhydrous character of the etch, is obtained with an anodic current density of 10  $\text{mA}/\text{cm}^2$  for 15 s. After anodization, the sample was rinsed in pure methanol, removed from the glovebox, dried, and characterized using FTIR and photoluminescence spectroscopies.

Warntjes et al.<sup>7</sup> make two key observations: They (1) find that the visible PL spectrum blue shifts upon methoxylation by at least 10 nm from that of hydrogenated PS and (2) obtain evidence for methyl ( $\nu(\text{CH}_3)$ ) and  $\nu(\text{SiOC})$  infrared bands, suggesting the grafting of  $\text{OCH}_3$  units and the formation of  $\text{SiOCH}_3$  constituencies. After methoxylation, Warntjes et al.<sup>7</sup> observe that their initially prepared PS surface is modified to exhibit less intense and broadened Si–H vibrational features compared with those characteristic of the unmodified surface. While these authors<sup>7</sup> suggest that there is little evidence for oxidized Si–H species (back-bonded oxygen), the *asymmetric broadening* of the nominal 2090, 2110, and 2140  $\text{cm}^{-1}$  Si–H frequencies in the 2150–2250  $\text{cm}^{-1}$  region is open to alternate interpretation. New bands appear at 2945 and 2840  $\text{cm}^{-1}$  ( $\nu(\text{CH}_3)$ ), 1190  $\text{cm}^{-1}$  ( $\rho(\text{CH}_3)$ ), 1085  $\text{cm}^{-1}$  ( $\nu_{\text{as}}\text{SiOC}$ ), and 800  $\text{cm}^{-1}$  ( $\nu_{\text{s}}\text{SiOC}$ ), which are assigned as indicated. The observed features are those that suggest the grafting of  $-\text{OCH}_3$  units onto the PS surface as strongly evidenced by the association of the 2840  $\text{cm}^{-1}$  band with the 1190, 1085, and 800  $\text{cm}^{-1}$  bands, a sequence highly characteristic of  $\text{SiOCH}_3$  units.<sup>22</sup> The modified PS layers also exhibit an increased luminescence (Figure 1) and a blue shift of the emission as compared to the luminescence recorded prior to modification.

The methoxylated PS surface thus exhibits improved optical characteristics with an increased photoluminescence efficiency and blue shift of the emission. Its stability against aging is improved versus that of the hydrogenated surface but does not

reach the stability of anodically oxidized PS.<sup>7</sup> Because this derivatization produces desired characteristics that may, in fact, be useful for sensor technology, it is appropriate to employ detailed quantum chemical modeling as a means for evaluating those parameters that enhance the potential for PL stability and an increased quantum yield for light emission and their plausible correlation with a modification of silicon oxyhydride fluorophors on a PS surface.

### Nature of the Quantum Calculations

To assess the nature of the silicon oxyhydrides, their methoxy-substituted counterparts, and their potential role as the source of the luminescence from a modified PS surface, we have extended previous studies<sup>23,24</sup> of the molecular electronic structure of silanone ( $\text{Si}(\text{O})\text{H}_2$ ), the OH (for H)-substituted silanoic ( $\text{Si}(\text{O})\text{H}(\text{OH})$ ) and silycic ( $\text{Si}(\text{O})(\text{OH})_2$ ) acids, and  $\text{Si}(\text{O})\text{H}(\text{OSiH}_3)$ ,  $\text{Si}(\text{O})(\text{OH})\text{SiH}_3$ ,  $\text{Si}(\text{O})\text{SiH}_3(\text{OSiH}_3)$ , and  $\text{SiO}(\text{SiH}_3)_2$  as models<sup>15,19,21,36</sup> for the sites present on the surface of an etched silicon wafer. We have employed both ab initio molecular orbital theory and density functional theory (DFT-ground-state singlets) using the program systems DGauss<sup>25</sup> (DFT calculations) and Gaussian 94<sup>26</sup> (ab initio MO calculations). With the molecules  $\text{Si}(\text{O})\text{H}_2$ ,  $\text{Si}(\text{O})\text{H}(\text{OH})$ ,  $\text{Si}(\text{O})(\text{OH})_2$ ,  $\text{Si}(\text{O})\text{H}(\text{OSiH}_3)$ ,  $\text{Si}(\text{O})\text{H}(\text{SiH}_3)$ ,  $\text{Si}(\text{O})(\text{OH})(\text{SiH}_3)$ ,  $\text{Si}(\text{O})\text{SiH}_3(\text{OSiH}_3)$ , and  $\text{Si}(\text{O})(\text{SiH}_3)_2$  we attempted to evaluate<sup>19</sup> the types of sites that might be present on a hydrogen-passivated silicon surface<sup>27</sup> undergoing oxidation. Further calculations were carried out on the Si XYZ compounds, where the XYZ vary through the series from  $\text{SiH}_3$  to  $\text{Si}(\text{OH})_3$ .<sup>19</sup> Although cluster models such as these do not include the long-range Coulomb effects present in the bulk, they can provide clear insights into the effect of changing the functional groups that might be attached at the silicon. Here, we extend these calculations to modify the silanone-based oxyhydrides by introducing methyl groups to replace hydrogen and  $\text{SiH}_3$  constituencies.

Optimized geometries were calculated at the DFT level for the ground-state singlet and in some cases for the lowest excited triplet state silanones using a polarized triple- $\zeta$  basis set.<sup>28</sup> Second derivative calculations demonstrate that these structures represent minima.<sup>29</sup> These optimum geometries were then used in molecular orbital calculations at the MP2 level<sup>30</sup> with a polarized double- $\zeta$  basis set.<sup>31</sup> Geometries were reoptimized at the MP2/DZP level, and frequency calculations were done for several of these optimized geometries. To evaluate corrections to the singlet–triplet separations determined at the MP2/DZP level, higher order correlation corrections were done on  $\text{Si}(\text{O})\text{H}_2$  at the optimized geometries. These calculations were done at the CCSD(T) level<sup>32</sup> with a triple- $\zeta$  basis set<sup>33</sup> augmented by two sets of polarization functions on all atoms and by f functions on the heavy atoms.

### Quantum Chemical Modeling

The most relevant results of our quantum chemical calculations are summarized in Tables 1 and 2. In Table 1, we summarize the SiO bond lengths calculated at the MP2/DZP level for the ground-state singlets and lowest-lying excited-state triplets of the model silanone- and methyl-substituted silanone-based oxyhydride compounds which we have considered. The corresponding Si XYZ compounds from  $\text{SiH}_3$  to  $\text{Si}(\text{OH})_3$ <sup>19</sup> possess excited states whose lowest-lying transitions all lie far into the ultraviolet region. These excited states are not accessible to the light sources used to study the photoluminescence from either substituted or unmodified PS surfaces and therefore are not considered further. Table 1 demonstrates that

**TABLE 1: Si=O Bond Lengths (Å) for Silanones and Methyl-Substituted Silanones at the MP2/DZP Level of Description**

molecule	$r(\text{SiO})$ singlet	$r(\text{SiO})$ triplet	$\Delta r(\text{SiO})$
Si(O)H <sub>2</sub>	1.545	1.700 <sup>a</sup>	0.155
Si(O)(SiH <sub>3</sub> ) <sub>2</sub>	1.560	1.681	0.121
Si(O)H(SiH <sub>3</sub> )	1.553	1.695	0.142
Si(O)H(CH <sub>3</sub> )	1.545	1.705	0.160
Si(O)(CH <sub>3</sub> ) <sub>2</sub>	1.547	1.709	0.162
Si(O)(CH <sub>3</sub> )(SiH <sub>3</sub> )	1.552	1.699	0.147
Si(O)H(OH) <sup>b</sup>	1.537	1.709	0.172
Si(O)SiH <sub>3</sub> (OH)	1.543	1.712	0.169
Si(O)CH <sub>3</sub> (OH)	1.540	1.715	0.175
Si(O)H(OSiH <sub>3</sub> )	1.537	1.708	0.171
Si(O)SiH <sub>3</sub> (OSiH <sub>3</sub> )	1.543	1.712	0.169
Si(O)CH <sub>3</sub> (OSiH <sub>3</sub> )	1.540	1.713	0.173
Si(O)H(OCH <sub>3</sub> )	1.538	1.713	0.175
Si(O)SiH <sub>3</sub> (OCH <sub>3</sub> )	1.544	1.716	0.172
Si(O)CH <sub>3</sub> (OCH <sub>3</sub> )	1.541	1.718	0.177
Si(O)(OH) <sub>2</sub>	1.536	1.709	0.173
Si(O)(OH)(OCH <sub>3</sub> )	1.537	1.704	0.167
Si(O)(OSiH <sub>3</sub> ) <sub>2</sub>	1.537	1.708	0.171
Si(O)(OCH <sub>3</sub> ) <sub>2</sub>	1.538	1.715	0.177
Si(O)(OSiH <sub>3</sub> )(OCH <sub>3</sub> )	1.537	1.715	0.178

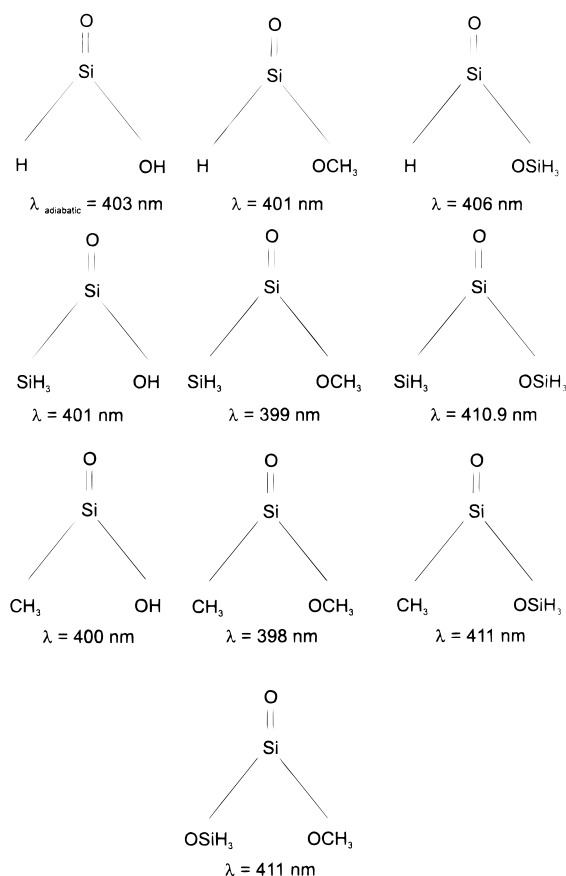
<sup>a</sup> Bond length for the excited singlet is 1.705 Å. <sup>b</sup> Bond lengths for HO–Si–OH silylene are 1.670 Å for the ground-state singlet and 1.680 Å for the excited triplet.

**TABLE 2: Ground-State Singlet–Excited-State Energy Separations for Silanones, Methyl-Substituted Silanones, and Silylenes**

molecule	$\Delta E(\text{S–T})$ (kcal/mol)	$\Delta E(\text{S–T})$ (eV)	$\sim \lambda_{\text{adiabatic}}$ (nm)
Si(O)H <sub>2</sub>	60.1	2.60	475
Si(O)(SiH <sub>3</sub> ) <sub>2</sub>	53.9	2.34	530
Si(O)H(SiH <sub>3</sub> )	57.3	2.48	499
Si(O)H(CH <sub>3</sub> )	63.0	2.73	454
Si(O)(CH <sub>3</sub> ) <sub>2</sub>	60.9	2.64	469
Si(O)(CH <sub>3</sub> )(SiH <sub>3</sub> )	71.6	3.10	399
Si(O)H(OH)	70.9	3.07	403
Si(O)SiH <sub>3</sub> (OH)	71.3	3.09	401
Si(O)CH <sub>3</sub> (OH)	71.9	3.12	398
Si(O)H(OSiH <sub>3</sub> )	70.4	3.05	406
Si(O)SiH <sub>3</sub> (OSiH <sub>3</sub> )	69.6	3.02	411
Si(O)CH <sub>3</sub> (OSiH <sub>3</sub> )	69.6	3.02	411
Si(O)H(OCH <sub>3</sub> )	71.3	3.09	401
Si(O)SiH <sub>3</sub> (OCH <sub>3</sub> )	71.6	3.10	399
Si(O)CH <sub>3</sub> (OCH <sub>3</sub> )	71.8	3.11	398
Si(O)(OH) <sub>2</sub>	71.1	3.08	402
Si(O)(OH)(OCH <sub>3</sub> )	71.9	3.12	398
Si(O)(OSiH <sub>3</sub> ) <sub>2</sub>	67.1	2.91	426
Si(O)(OCH <sub>3</sub> ) <sub>2</sub>	70.9	3.07	403
Si(O)(OSiH <sub>3</sub> )(OCH <sub>3</sub> )	69.6	3.02	411
HSiOH	38.4	1.66	744
HOSiOH	64.2	2.78	445
SiH <sub>3</sub> OSiH <sub>3</sub>	67.4	2.92	425

a significant change accompanies the silanone transitions to the excited triplet state with which we associate the triplet exciton identified by Stutzmann and co-workers.<sup>15–17</sup> This transition produces a considerable lengthening of the SiO bond.<sup>5,19,21,36</sup> In contrast, the silylene isomers (ref 19) produce no such change upon transition to their low-lying triplet state.

The data in Table 2 indicate the calculated singlet–triplet separations for a number of compounds that would appear to be relevant to the modeling of a standard, methylated, or methoxylated PS surface. To focus on the effects of methoxylation, the data in Table 2 are distilled to a smaller group of silanones in Figure 2, where we summarize the adiabatic singlet–triplet energies and their corresponding associated transition wavelength. It is noteworthy that the locations of

**Figure 2.** Calculated wavelengths corresponding to the adiabatic excitation energies (Table 2) for the lowest triplet states of several silanone-based silicon oxyhydrides. See also ref 19.

the unsaturated silanone-based silicon oxyhydride excited triplet states and the known peak wavelength of the porous silicon (PLE) excitation spectrum ( $\sim 350$  nm)<sup>34</sup> bear a clear resemblance to the known singlet–triplet splittings of the low-lying silicon monoxide intercombination band systems.<sup>35</sup> The large change in the SiO bond lengths indicated in Table 1, in turn, produces a large shift in the excited-state potentials relative to the ground state. This location of the ground- and excited-state potentials promotes optical pumping high up the excited-state potential and a significant difference in the peak of the PLE excitation spectrum ( $\sim 350$  nm) and the observed PL emission range ( $\sim 600$ – $850$  nm (orange) (see Figure 3)). While the data are consistent with excitation pumping high up the excited triplet state manifold, it is also clear that there will be subsequent rapid nonradiative vibrational relaxation through the excited triplet manifold before the emission<sup>19,36</sup> of radiation.

There are additional striking aspects of the data in Tables 1 and 2. First, we note that whenever an OH, OCH<sub>3</sub>(OR), or OSiH<sub>3</sub>(OR) group is bound to the silicon–oxygen bond, the change,  $\Delta r(\text{SiO})$ , in transition is consistently on the order of 0.17–0.175 Å. Further, an additional OH group does little to affect the differential change in the bond length accompanying the singlet–triplet transition. In the absence of an –OH or –OR group, this change in bond length is smaller, decreasing from 0.162 Å for Si(O)(CH<sub>3</sub>)<sub>2</sub> to 0.121 Å for Si(O)(SiH<sub>3</sub>)<sub>2</sub>. These are differences that would appear to be associated with an –OR versus –R group bonding to the silicon. Further, we note the very similar adiabatic energy differences ( $\Delta E \approx 3.05 \pm 0.05$  eV) that, with only one exception, (Si(O)(OSiH<sub>3</sub>)<sub>2</sub>), characterize the singlet–triplet transitions where an –OH or –OR group is bound to the silicon oxide bond. The shift of the excited triplet

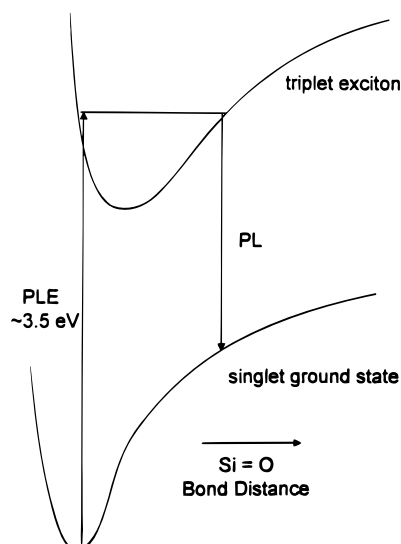


**Figure 3.** Rough schematic of silicon oxyhydride ground-state singlet and excited-state triplet potentials indicating the origin of the substantial difference in photoluminescence excitation (PLE) and subsequent photoluminescence (PL) emission energies.

state relative to the ground-state singlet suggests that the maximum at  $\sim 3.5$  eV for the PLE excitation spectrum is quite consistent with a silanone-based oxyhydride, containing an  $-\text{OH}$  or  $-\text{OR}$  group, on the PS surface. It is also appropriate that we contrast the virtually identical energy increments for those silanones containing an  $-\text{OR}$  group to the much lower energy differences associated with the series  $\text{Si}(\text{O})\text{H}_2$ , ( $\Delta r = 0.155$  Å),  $\text{Si}(\text{O})\text{H}(\text{SiH}_3)$  ( $\Delta r = 0.142$  Å), and  $\text{Si}(\text{O})(\text{SiH}_3)_2$  ( $\Delta r = 0.121$  Å), where also we indicate the smaller changes in the SiO bond length upon transition. Further, we observe a clear trend in the change,  $\Delta r(\text{SiO})$ , as we progress through the series  $\text{Si}(\text{O})-(\text{CH}_3)_2$  ( $\Delta r = 0.162$  Å),  $\text{Si}(\text{O})\text{H}(\text{CH}_3)$  (0.160 Å),  $\text{Si}(\text{O})\text{H}_2$  (0.155 Å),  $\text{Si}(\text{O})(\text{CH}_3)(\text{SiH}_3)$  (0.147 Å),  $\text{Si}(\text{O})\text{H}(\text{SiH}_3)$  (0.142 Å), and  $\text{Si}(\text{O})(\text{SiH}_3)_2$  (0.121 Å). This change in transition is most likely associated with the electron-withdrawing character of the methyl radical versus the electron-donating character of the silyl radical.

### Changes in Photoluminescence upon Methyl Substitution

The calculated structures outlined in Figure 2 indicate the changes to be expected as one converts the  $\text{O}=\text{Si}-\text{OH}$  and  $\text{O}=\text{Si}-\text{OSiH}_3$  constituencies which we have previously considered,<sup>19,36</sup> as they are plausibly associated with an unmodified PS surface, to an  $\text{O}=\text{Si}-\text{OCH}_3$  fluorophore upon methoxylation. We discern that the predicted change in adiabatic energy commensurate with a blue shift in the visible PL spectrum is not readily associated with the conversion of a hydroxyl group ( $-\text{OH}$ ) to an  $-\text{OCH}_3$  functional group. This change, if ascribed to a change in functionality, would appear to be associated with the conversion of an  $-\text{OSiH}_3$  unit to  $-\text{OCH}_3$ , a modification that will produce a shift consistent with the observations of Warntjes et al.,<sup>7</sup> as indicated in Figure 1. Further, any conversion of an  $-\text{OH}$  or  $-\text{OSiH}_3$  to a methyl ( $\text{CH}_3$ ) constituency will likely (Table 2) result in a substantial red shift in the PL spectrum, clearly inconsistent with experimental observation.

Calculated infrared spectral frequencies for  $\text{Si}(\text{O})\text{SiH}_3(\text{OSiH}_3)$  and the methyl-substituted  $\text{Si}(\text{O})\text{SiH}_3(\text{OCH}_3)$ , for the frequency range covered by the FTIR studies of Warntjes et al., are given in Tables 3 and 4. While the calculated values in these tables are for the silanone-based molecules, they provide an indication of the frequencies that should be associated with the surface-bound fluorophores  $-\text{Si}(\text{O})(\text{OSiH}_3)$  and  $-\text{Si}(\text{O})(\text{OCH}_3)$ . In the

**TABLE 3: Calculated Frequencies ( $\nu \geq 450$   $\text{cm}^{-1}$ )<sup>a,b</sup> for**

$\nu$ ( $\text{cm}^{-1}$ )	$I$ (km/mol)	assignment
2198	47	(SiH <sub>3</sub> )–Si (Si–H) stretch
2186	88	(SiH <sub>3</sub> )–O (Si–H) stretch
2178	85	(SiH <sub>3</sub> )–O (Si–H) stretch
2177	71	(SiH <sub>3</sub> )–O (Si–H) stretch
2172	53	(SiH <sub>3</sub> )–Si (Si–H) stretch
2167	28	(SiH <sub>3</sub> )–Si (Si–H) stretch
1220	175	Si=O stretch
1031	382	Si–O–Si asymmetric stretch
910	287	SiH <sub>3</sub> O (inv) bend
898	34	SiH <sub>3</sub> O (inv) bend
895	37	SiH <sub>3</sub> O (inv) bend
892	28	SiH <sub>3</sub> –Si bend
889	15	SiH <sub>3</sub> –Si bend
803	253	SiH <sub>3</sub> (inv) bend
691	39	SiH <sub>3</sub> (O) rock
677	39	SiH <sub>3</sub> (O) rock
619	5	Si–O–Si symm stretch
507	4	SiH <sub>3</sub> (Si) wag
483	21	SiH <sub>3</sub> (Si) wag
452	30	Si–Si stretch + Si–O–Si bend

<sup>a</sup> Frequency range of FTIR spectra exceeds 450  $\text{cm}^{-1}$ . <sup>b</sup> Calculations at MP2/DZP level.

**TABLE 4: Calculated Frequencies ( $\nu \geq 450$   $\text{cm}^{-1}$ )<sup>a,b</sup> for**

$\nu$ ( $\text{cm}^{-1}$ )	$I$ (km/mol)	assignment
3069	16	C–H stretch
3055	11	C–H stretch
2966	47	C–H stretch
2196	47	SiH stretch
2172	51	SiH stretch
2167	29	SiH stretch
1421	15	CH <sub>3</sub> bend
1417	12	CH <sub>3</sub> bend
1393	4	CH <sub>3</sub> bend
1218	146	Si=O stretch
1143	44	CH <sub>3</sub> rock + C–O stretch
1113	0	CH <sub>3</sub> rock + C–O stretch
1093	202	C–O–Si stretch
888	20	SiH <sub>3</sub> bend
881	18	SiH <sub>3</sub> bend
809	97	SiH <sub>3</sub> bend
763	115	Si–O stretch + SiH <sub>3</sub> bend
502	9	SiH <sub>3</sub> wag
480	17	SiH <sub>3</sub> wag
478	17	SiH <sub>3</sub> wag

<sup>a</sup> Frequency range of FTIR spectra exceeds 450  $\text{cm}^{-1}$ . <sup>b</sup> Calculations at MP2/DZP level.

region near 500  $\text{cm}^{-1}$ , we expect to observe features associated with an SiH<sub>3</sub> wag. There is a clear indication of these features in the spectra of Warntjes et al. (Figure 1, ref 7). The calculated SiH<sub>x</sub> and oxygen-backed SiH<sub>x</sub> silicon–hydrogen bands (Table 3) and the higher frequency C–H stretch bands (Table 4), determined with good accuracy, are clearly in good correlation with experimental observation. Both the SiH<sub>3</sub> (Table 3) and CH<sub>3</sub> (Table 4) rocking vibrations appear to be accurately predicted, as is the SiH<sub>3</sub>O (inv) bend. However, the CH<sub>3</sub> bend, determined experimentally, is found at a considerably lower frequency than the calculated value (Table 4). Most important for our considerations is the calculation of the Si=O stretch

## (100) Silicon Surface Reactions

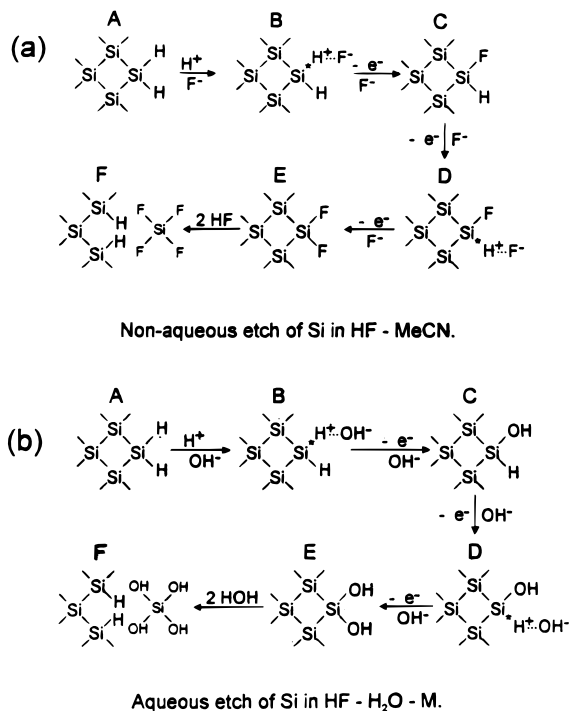


**Figure 4.** Reaction mechanisms for dissolution and silicon fluoride and silicon hydroxide (oxyhydride) bond formation in nonaqueous and aqueous HF etch solutions.

vibrations in a frequency range commensurate with both the untreated and methoxylated porous silicon spectra observed by Warntjes et al.<sup>7</sup> (Figure 1, ref 7). The data presented by Warntjes et al.<sup>7</sup> coupled with our quantum chemical calculations would indicate not only oxide formation but also the mild oxidation of SiH<sub>x</sub> bonds in both their untreated and methoxylated PS samples.<sup>21</sup>

Warntjes et al.<sup>7</sup> have noted that silicon, as it is oxidized in methanol, should undergo spontaneous dissolution to form soluble tetramethoxysilane, in analogy with the mechanism for HF etching. This process is expected to proceed through the successive grafting of methoxy units (e.g., analogue of F atoms in HF; see the following) to the silicon atoms. However, dependent upon the experimental conditions, it might also be possible to graft methyl groups onto a hydrogenated silicon surface to substitute the silicon-hydrogen bonds, eventually forming the more easily removed tetramethylsilane.<sup>6</sup> These considerations cause us to consider the potential evolution of PS and its derivative surfaces as they undergo dissolution with change in experimental conditions.

### Etching and Photoluminescence Process

Several researchers have considered the reactions that describe the dissolution of silicon in an HF-containing electrolyte. The formation of the silicon oxyhydrides or their methyl derivative emitters<sup>5,36</sup> would appear to be consistent with the comparative and competitive mechanisms that have been suggested for silicon dissolution in aqueous and nonaqueous media.<sup>37,38</sup> Figure 4a outlines the cycle of suggested conversion steps in a nonaqueous etching process that provide the dissolution of silicon through the eventual formation of an SiF<sub>4</sub> leaving group. This process can be inhibited through the introduction of water, and in an aqueous medium, the competitive mechanism indicated in Figure

4b is thought to proceed through the formation of silicon hydroxide bonds, which might well result in the formation of surface-bound photoluminescent oxyhydrides.<sup>5,36</sup>

The nonaqueous etching process (Figure 4a) in an HF/MeCN solution is thought to form an initial dihydride surface (A) where *ab initio* calculations<sup>40</sup> have shown that kinetic rather than purely thermodynamic factors are responsible for hydride passivation. The initial dihydride surface, which can be considered either a (100) surface or the kink site of a (111) surface, is thought to be stable in solution.<sup>37</sup> This surface does not appear to be photoluminescent,<sup>5,36</sup> consistent with quantum chemical calculations<sup>19</sup> and experimental evaluations<sup>41</sup> of SiH<sub>x</sub> excited states. The reaction sequence with HF is thought to be hole initiated (B), producing a proton and a silicon radical.<sup>37-39</sup> After electron ejection into the silicon conduction band, facilitated by the ready oxidation of silicon, the positively charged silicon is thought to be complexed by a fluoride ion (C). This process is thought to continue as the high electronegativity of fluoride in the silicon fluoride bond destabilizes the adjacent Si-H bond, which is then more susceptible to oxidation through electron injection or hole consumption (D). In the absence of water, a fourth oxidative step (E) can take place as the addition of fluoride to the oxidized silicon further destabilizes the Si-Si bonds. The polarity of the two Si-F bonds can facilitate the further addition of HF and the final dissolution of SiF<sub>4</sub>, which dissolves as the silicon hexafluoride.

As Gerischer et al. have suggested,<sup>38</sup> and we have previously outlined,<sup>42</sup> the presence of water in the etch solution should inhibit the anhydrous dissolution process. We suggest that water can interact in at least three different ways with a silicon surface to produce Si=O, Si-O-Si, and Si-OH bonding units.<sup>6</sup> Similarly, anhydrous methanol can alter the etch cycle.

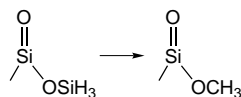
Within the suggested mechanism for the steady-state oxidation of a hydrogen-coated silicon surface in an aqueous electrolyte (Figure 4b), the hydrolysis of silicon (B, C) can compete favorably with fluorination, as oxide bonds are readily formed during silicon anodization.<sup>37,38</sup> The hydrolysis of the silicon radical (B) represents an important alternate oxidation route, as the presence of water can lead to the formation of an Si-OH bond. Given a silicon surface that is not completely hydride decorated, we may consider also the possible formation of the Si=O bond or the Si-O-Si moiety through a concerted reaction of the water molecule on the silicon surface, the combination of water reactions then producing an -Si(O)(OH) or -Si(O)-(OSiH<sub>3</sub>) oxyhydride fluorophor. In Figure 4b, the formation of the hydroxide bond alters and decreases the reactivity of the remaining Si-H bond (C), which is now less susceptible to electron injection or nucleophilic attack. The lower induced polarization of the hydroxide group also weakens the Si-Si bonds to a lesser extent, signaling an increased stability for the hydroxy intermediates indicated in C and E. With available silicon sites, the introduction of water, which can lead to the formation of silicon oxide and hydroxide bonds as opposed to the silicon fluoride bond, thus signals the creation of silicon oxyhydride surface entities and, within this process, provides additional stability. This behavior is in close correlation with the observations we have outlined<sup>5,6,42</sup> as we perturb the *in situ* nonaqueous etching environment through the introduction of water, whose presence appears to enhance and stabilize the

formation of the PL emission from PS.<sup>42</sup> Here, it is likely that we facilitate the PL process by stabilizing a surface-bound silicon oxyhydride which can fluoresce in parallel and competition with the process of silicon dissolution. This, of course, inhibits the dissolution process. We suggest that, in an aqueous HF/H<sub>2</sub>O (doubly deionized water) etching solution, the competitive branching between hydroxide and fluoride formation is in large part responsible for the formation of photoluminescent emitters in direct competition with dissolution and SiO<sub>2</sub> formation. The judicious manipulation of the etching solution might therefore be used to create means for producing more efficient photoluminescent emitters. The considerations that we have outlined for the formation of the silanol functional group also apply to the formation of the Si—OCH<sub>3</sub> moiety (analogue of C, E, Figure 4b), which should, in fact, make the remaining SiH bonds even less susceptible to electron injection or nucleophilic attack.

If anhydrous methanol is now used to etch a PS surface, its introduction can modify the "limiting" mechanisms defined in Figure 4 in significant ways. We first consider whether methanol replaces the water molecule as CH<sub>3</sub>O<sup>−</sup>H<sup>+</sup>. Here, as the silanol moiety will be substituted to an SiOCH<sub>3</sub> constituency, the anticipated shift in the PL emission spectrum will be quite small. However, the methyl substitution will stabilize and enhance the photoluminescence. If we expand these mechanistic evaluations to consider the formation of a silanone-based oxyhydride and the oxyhydride surface unit is, in fact, —Si(O)(OSiH<sub>3</sub>), we suggest that its subsequent conversion to —Si(O)(OCH<sub>3</sub>) will produce not only a stabilization but also a blue shift of the PL. This, of course, would appear to be in excellent agreement with the observations of Warntjes et al.<sup>7</sup> The final dissolution product tetramethoxysilane will replace tetrahydroxysilane in Figure 4b,F. If, however, a portion of the methanol constituency interacts as CH<sub>3</sub><sup>+</sup>OH<sup>−</sup>, the reaction sequence outlined in Figure 4 will have a destabilizing effect on the silicon surface as hydrogen bonds are converted to Si—CH<sub>3</sub> constituencies. This should facilitate dissolution in subsequent mechanistic cycles. The experimental evidence thus far would suggest that, at least in the experiments of Warntjes et al.,<sup>7</sup> the former interaction, as CH<sub>3</sub>O<sup>+</sup>H<sup>−</sup>, is dominant.

## Summary and Conclusion

By evaluating the low-lying triplet—singlet transitions of the silanone-based silicon oxyhydrides we are able to suggest a plausible explanation for the blue shift and enhanced stability inherent to a porous silicon surface that has been subsequently methoxylated. We suggest that if the blue shift is due to a change in the molecular electronic structure of a surface bound silicon oxyhydride, it likely results from the conversion



**Acknowledgment.** We acknowledge financial support from the Office of the President at Georgia Institute of Technology under the auspices of the Focused Research Program. The quantum chemical calculations were performed under the auspices of the Office of Basic Energy Sciences, U.S. Department of Energy, under Contract DE-AC06-76RLO 1830 with Battelle Memorial Institute, which operates the Pacific Northwest Laboratory.

## References and Notes

- (1) Canham, L. T. *Appl. Phys. Lett.* **1990**, *57*, 1046.
- (2) (a) Kanemitsu, Y. *Phys. Rep.* **1995**, *263*, 1–92. (b) John, G. C.; Singh, V. A. *Phys. Rep.* **1995**, *263*, 93–152.
- (3) Prokes, S. M. *J. Mater. Res.* **1996**, *11*, 305.
- (4) Astrova, E. S.; Belov, S. V.; Lebedev, A. A.; Rermenjuk, A. D.; Rud, Yu, V. *Thin Solid Films* **1995**, *255*, 196–199.
- (5) Gole, J. L.; Dixon, D. A. On the Transformation, Green to Orange-Red, of a Porous Silicon Photoluminescent Surface. *J. Phys. Chem.* **1998**, *133*, 33.
- (6) Dudel, F.; Seals, L.; Gole, J. L.; Bottomley, L.; Reiger, M. On the Correlation of Aqueous and Nonaqueous In Situ and Ex-Situ Photoluminescent Emissions from Porous Silicon. *J. Electrochem. Soc.*, submitted.
- (7) Warntjes, M.; Veillard, C.; Ozanam, F.; Chazalviel, J. N. *J. Electrochem. Soc.* **1995**, *142*, 4138.
- (8) (a) Koch, F.; Petrova-Koch, V.; Muschik, T. *J. Lumin.* **1993**, *57*, 271. (b) Koch, F.; Petrova-Koch, V.; Muschik, T.; Nikolov, A.; Gavrilenko, V. *Mater. Res. Soc. Symp. Proc.* **1993**, *283*, 197. (c) Koch, F. *Mater. Res. Soc. Symp. Proc.* **1993**, *298*, 222.
- (9) Chazalviel, J. N. *J. Electroanal. Chem.* **1987**, *233*, 37.
- (10) See, for example: Calcott, P. D. J.; Nash, K. J.; Canham, L. T.; Kane, M. J.; Brumhead, D. J. *Phys. Condens. Matter* **1993**, *5*, L91–98.
- (11) Calcott, P. D. J.; Nash, K. J.; Canham, L. T.; Kane, M. J.; Brumhead, D. J. *Lumin.* **1993**, *57*, 257.
- (12) Nash, K. J.; Calcott, P. D. J.; Canham, L. T.; Needs, R. *J. Phys. Rev. B* **1995**, *51*, 17698.
- (13) Xie, Y. H.; Wilson, W. L.; Ross, F. M.; Mucha, J. A.; Fitzgerald, E. A.; Macauley, J. M.; Harris, T. D. *J. Appl. Phys.* **1992**, *71*, 2403.
- (14) (a) Prokes, S.; Glembocki, O. J.; Bermudez, V. M.; Kaplan, R.; Friedersdorf, L. E.; Pearson, P. C. *Phys. Rev. B* **1992**, *45*, 13788. (b) Prokes, S. M. *J. Appl. Phys.* **1993**, *73*, 407.
- (15) Fuchs, H. D.; Rosenbauer, M.; Brandt, M. S.; Ernst, S.; Finkbeiner, S.; Stutzmann, M.; Syassen, K.; Weber, J.; Queisser, H. J.; Cardona, M. Visible Luminescence from Porous Silicon and Siloxene: Recent Results. *Mater. Res. Soc. Proc.* **1993**, *283*, 203.
- (16) Stutzmann, M.; Brandt, M. S.; Rosenbauer, M.; Fuchs, H. D.; Finkbeiner, S.; Weber, J.; Deak, P. Luminescence and Optical Properties of Siloxene. *J. Lumin.* **1993**, *57*, 321.
- (17) Brandt, M. S.; Stutzmann, M. Triplet Excitons in Porous Silicon and Siloxene. *Solid State Commun.* **1995**, *93*, 473.
- (18) Steckl, A. J.; Xu, J.; Mogul, H. C.; Prokes, S. M. *J. Electrochem. Soc.* **1995**, *142*, L69–71.
- (19) Gole, J. L.; Dixon, D. A. On the Nature of the Ultraviolet Pump Efficiency, Visible Light Emission, and Infrared Spectrum of a Porous Silicon Surface—The Potential Role of Silanones and Silylenes. *Phys. Rev. B*, in press.
- (20) See, for example: (a) Brus, L. E.; Szajowski, P. F.; Wilson, W. L.; Harris, T. D.; Schuppler, S.; Citrin, P. H. *J. Am. Chem. Soc.* **1995**, *117*, 2915. (b) Green, G. J.; Gole, J. L. *Chem. Phys.* **1985**, *100*, 133.
- (21) Gole, J. L.; Dixon, D. A. A Suggested Correlation between the Visible Photoluminescence and the Fourier Transform Infrared Spectrum of a Porous Silicon Surface. *J. Phys. Chem.* **1997**, *82*, 3125.
- (22) Lin-Vien, D.; Colthup, N. B.; Fateley, W. G.; Grasselli, J. G. *The Handbook of Infrared and Raman Characteristic Frequencies of Organic Molecules*; Academic Press: San Diego, CA, 1991; pp 70–71, 258–259, 410.
- (23) Glinski, R. J.; Gole, J. L.; Dixon, D. A. *J. Am. Chem. Soc.* **1985**, *107*, 5891.
- (24) Dixon, D. A.; Gole, J. L. *Chem. Phys. Lett.* **1986**, *125*, 179.
- (25) (a) Andzelm, J.; Wimmer, E.; Salahub, D. R. In *The Challenge of d and f Electrons: Theory and Computation*; Salahub, D. R., Zerner, M. C., Eds.; ACS Symposium Series 394; American Chemical Society: Washington, DC, 1989; p 228. (b) Andzelm, J. In *Density Functional Theory in Chemistry*; Labanowski, J., Andzelm, J., Eds.; Springer-Verlag: New York, 1991; p 155. (c) Andzelm, J. W.; Wimmer, E. *J. Chem. Phys.* **1992**, *96*, 1280.
- (26) Frisch, M. J.; Trucks, G. W.; Schlegel, H. B.; Gill, P. M. W.; Johnson, B. G.; Robb, M. A.; Cheeseman, J. R.; Keith, T.; Petersson, G. A.; Montgomery, J. A.; Raghavachari, K.; Al-Laham, M. A.; Zakrzewski, V. G.; Ortiz, J. V.; Foresman, J. B.; Cioslowski, J.; Stefanov, B. B.; Nanayakkara, A.; Challacombe, M.; Peng, C. Y.; Ayala, P. Y.; Chen, W.; Wong, M. W.; Andres, J. L.; Replogle, E. S.; Gomperts, R.; Martin, R. L.; Fox, D. J.; Binkley, J. S.; Defrees, D. J.; Baker, J.; Stewart, J. P.; Head-Gordon, M.; Gonzales, C.; Pople, J. A. *Gaussian 94*, Revision B.2; Gaussian, Inc.: Pittsburgh, PA, 1995.
- (27) Prokes, S. M. Electrochemical Society Interface, Summer 1994; pp 41–43.
- (28) Godbout, N.; Salahub, D. R.; Andzelm, J.; Wimmer, E. *Can. J. Chem.* **1992**, *70*, 560.
- (29) Komornicki, A.; Fitzgerald, G. *J. Phys. Chem.* **1993**, *98*, 1398, and references therein.

- (30) (a) Moller, C.; Plesset, M. S. *Phys. Rev.* **1934**, *46*, 618. (b) Pople, J. A.; Binkely, J. S.; Seeger, R. *Int. J. Quantum Chem. Symp.* **1976**, *10*, 1.
- (31) Dunning, T. H.; Hay, P. J., Jr. In *Methods of Electronic Structure Theory*; Schaefer, H. F., III, Ed.; Plenum Press: New York, 1977; Chapter 1. McLean, A. D.; Chandler, G. S. *J. Chem. Phys.* **1980**, *72*, 5639.
- (32) (a) Bartlett, R. J. *J. Phys. Chem.* **1989**, *93*, 1697. (b) Kucharski, S. A.; Bartlett, R. J. *Adv. Quantum Chem.* **1986**, *18*, 281. (c) Bartlett, R. J.; Stanton, J. F. In *Reviews of Computational Chemistry, Vol. V*; Lipkowitz, K. B., Boyd, D. B., Eds.; VCH Publishers: New York, 1995; Chapter 2, p 65.
- (33) For the Si basis see: Dobbs, K. D.; Dixon, D. A. *J. Phys. Chem.* **1994**, *98*, 5290. For O and H, see: Dobbs, K. D.; Dixon, D. A.; Kormonicki, A. *J. Chem. Phys.* **1993**, *98*, 8852.
- (34) See, for example: Brus, L. E.; Szajowski, P. F.; Wilson, W. L.; Harris, T. D.; Schuppler, S.; Citrin, P. H. *J. Am. Chem. Soc.* **1995**, *117*, 2915.
- (35) See, for example: Green, G. J.; Gole, J. L. *Chem. Phys.* **1985**, *100*, 133.
- (36) Gole, J. L.; Dudel, F. P.; Grantier, D.; Dixon, D. A. On the Origin of Porous Silicon Photoluminescence—Evidence for a Surface Bound Oxyhydride-Like Emitter. *Phys. Rev. B* **1997**, *36*, 2137.
- (37) See, for example, discussions in: Propst, E. K.; Kohl, P. A. The Electrochemical Oxidation of Silicon and Formation of Porous Silicon in Acetonitrile. *J. Electrochem. Soc.* **1994**, *141*, 1006.
- (38) Gerischer, H.; Allongue, P.; Kieling, V. C. The Mechanism of the Anodic Oxidation of Silicon in Acidic Fluoride Solutions Revisited. *Ber. Bunsen-Ges. Phys. Chem.* **1993**, *97*, 753.
- (39) Lehmann, V.; Gosele, U. *Appl. Phys. Lett.* **1991**, *58*, 856.
- (40) Trucks, G. W.; Raghavachari, K.; Higashi, G. S.; Chabal, Y. J. Mechanism of HF Etching of Silicon Surfaces: A Theoretical Understanding of Hydrogen Passivation. *Phys. Rev. Lett.* **1990**, *65*, 504.
- (41) Jacox, M. E. *J. Phys. Chem. Ref. Data, Monograph No. 3*, **1994**, 127.
- (42) Dudel, F. P.; Gole, J. L. Stabilization of the Photoluminescence from Porous Silicon: The Competition Between Photoluminescence and Dissolution. *J. Appl. Phys.* **1997**, *42*, 802.